



Size Distribution and Water Soluble Ions of Ambient Particulate Matter on Episode and Non-episode Days in Southern Taiwan

Jiun-Horng Tsai¹, Jian-Hung Lin¹, Yung-Chen Yao², Hung-Lung Chiang^{3*}

¹ Department of Environmental Engineering, Sustainable Environmental Research Center, National Cheng-Kung University, Tainan, Taiwan

² Green Energy and Environment Research Laboratories, Industrial Technology Research Institute, Hsinchu, Taiwan

³ Department of Health Risk Management, China Medical University, Taichung, 40402, Taiwan

ABSTRACT

Distribution of inorganic ions at an urban/industrial/agricultural complex was investigated in southern Taiwan during particulate matter (PM) episode and non-episode periods, and the Micro Orifice Uniform Deposit Impactor (MOUDI) and nano-MOUDI were employed to take PM samples. In PM episode periods, the PM significantly increased in mass concentration and in the size ranges of 0.1–1.0 and 1.8–18 μm at the site. Sulfate, nitrate and ammonium were the dominant ionic species and contributed a large fraction of PM mass in different sizes. The nitrate concentration increase on episode days could be attributed to the increase of precursor gas- NO_2 concentration during these periods. In addition, SO_2 was significantly correlated to SO_4^{2-} in the nuclei mode ($\text{PM}_{0.1}$), which indicated that the gas had transferred into particulate matter. The molar equivalent ratio of $\{[\text{NO}_3^-] + [\text{SO}_4^{2-}]\}/[\text{NH}_4^+]$ was about 0.99 and revealed a high correlation that could indicate the presence of ammonium nitrate and ammonium sulfate in $\text{PM}_{1.0}$.

Keywords: Particulate matter; Size distribution; Gas precursors; Inorganic ions.

INTRODUCTION

Size distributions and chemical compositions of atmospheric aerosols play important roles in their toxicity, health effects, and visibility in urban areas (Ny and Lee, 2011; Han *et al.*, 2012). Many epidemiological studies have been published on the health risks associated with PM that is 10 μm or less in diameter (Health Effects Institute, 2003). Some results have also shown an association between PM and cardiovascular and respiratory disease (Oberdorster *et al.*, 1995; Burnett *et al.*, 1997; Ostro *et al.*, 2000; Brunekreef and Forsberg, 2005; Kan *et al.*, 2007). In America and Europe, epidemiologic studies of $\text{PM}_{2.5}$ have shown that long-term exposure is associated with an increase in mortality due to lung cancer and other cardiopulmonary diseases (Naess *et al.*, 2007; Brunekreef *et al.*, 2009; Boldo *et al.*, 2011). Therefore, PM characteristics such as size distribution and composition are important issues impacting the health effects of these atmospheric aerosols.

Numerous studies have measured ionic species in particulate matter (Lee *et al.*, 1999; Bari *et al.*, 2003a, b;

Pathak *et al.*, 2003, 2004; Pathak and Chan, 2005; Tsai *et al.*, 2005; Aneja *et al.*, 2006; Wang *et al.*, 2008; Hsieh *et al.*, 2009; Deshmukh *et al.*, 2011; Stone *et al.*, 2011). Zhao and Gao (2008) indicated that $\text{PM}_{1.8}$ made up 68% of PM_{10} mass concentrations, and water-soluble ions accounted for more than 50% of $\text{PM}_{1.8}$ mass concentrations, suggesting the significant role of water-soluble aerosol components in controlling the mass concentration of urban $\text{PM}_{1.8}$. But the mass size distribution of water-soluble inorganic and organic species is not well understood. Information about the distribution of sulfate, nitrate, ammonium and other species in aerosol is still lacking. Besides organic species, sulfate, nitrate and ammonium were the dominant components of water-soluble ions in PM (Aneja *et al.*, 2006; Hsieh *et al.*, 2009; Li *et al.*, 2009; Lin *et al.*, 2009; Shen *et al.*, 2009; Katzman *et al.*, 2010; Deshmukh *et al.*, 2011; Plaza *et al.*, 2011; Shen *et al.*, 2011; Zhao *et al.*, 2011). In the South Coast Air Basin, California, USA, up to 80% of nitrate and ammonium in fine particles was formed from precursor gas, and most of it came from mobile sources such as diesel and gasoline engines (Ying and Kleeman, 2006). Han *et al.* (2008) showed that ionic constituents accounted for 35–60% of $\text{PM}_{2.5}$ mass in industrial and urban cities of Korea, and sulfate and nitrate were the major ionic species. Plaza *et al.* (2011) indicated that the sulfate and ammonium mass was concentrated in accumulation mode, from 0.18–0.56 μm , and nitrate concentration was higher in coarse

* Corresponding author. Tel.: 886-4-22079685;
Fax: 886-4-22079687
E-mail address: hlchiang@mail.cmu.edu.tw

mode than in accumulation mode in the urban area of Madrid. Therefore, the gas phase and condensation processes for secondary aerosol formation could be important mechanisms in the urban area of Madrid. Through photochemical reactions in the atmosphere, NO_x and SO_2 emitted from natural and artificial sources led to the formation of nitrate and sulfate (Buhr *et al.*, 1995; Hazi *et al.*, 2003; Pathak and Chan, 2005). Nitrate was primarily in the submicron and coarse modes (Zhuang *et al.*, 1999; Tsai and Kuo, 2006; Zhao and Gao, 2008). The size distribution of sulfate and ammonium in PM reveals a bi-modal distribution of two submicron modes (Cabada *et al.*, 2004) or one submicron and one supermicron mode (Tsai and Kuo, 2006). Therefore, source emissions, human activities, chemical reactions, and meteorological conditions could affect the size portion and composition of PM in urban, rural and industrial areas (Wang *et al.*, 2005; Hu *et al.*, 2010, Oh *et al.*, 2011).

Ammonia may easily transfer into the particulate phase as NH_4^+ through reaction in the atmosphere (Walker *et al.*, 2003; Plessow *et al.*, 2005). Natural and anthropogenic sources, including the fertilizer industry, agricultural fermentation, and farm animal waste, could be sources of NH_3 (Walker *et al.*, 2003; Plessow *et al.*, 2005). Sulfate and nitrate are major components in particulate mass, and they could react with ammonia or ammonium to form ammonium nitrate and ammonium sulfate in the particulate phase. Most studies have reported similar measurements of gases and ionic species in particulate matter, but few have measured all of the compounds in different size fractions. In addition, water-soluble ionic species contribute a large portion of particulate mass; therefore, this article focuses on the water-soluble ions in PM size distribution as an important issue for ambient air quality management. However, the elemental and carbonaceous contents are also important in PM constituents.

The water-soluble ionic species including anions (NO_3^- , SO_4^{2-} , Cl^- , F^- , NO_2^- , Br^-) and cations (NH_4^+ , Na^+ , K^+ , Ca^{2+} , Mg^{2+}) for particulate size distribution and gaseous pollutants (i.e., HNO_2 , HNO_3 , HCl , SO_2 , NH_3) were determined in southern Taiwan during episode and non-episode periods. Distributions of the various size ranges were measured by a Micro Orifice Uniform Deposition Impactor (MOUDI) and a Nano-MOUDI.

MATERIALS AND METHODS

Study Area and Sampling Site

The ambient aerosol particle measurements were taken at the Daliao ambient air quality monitoring station, which is part of the Taiwan Air Quality Monitoring Network established by the Taiwan Environmental Protection Administration (TEPA) in 1993. This monitoring station was located immediately downwind from the Kao-Ping (Kaohsiung-Pingtung) ambient air quality basin, where the air quality has been the worst in Taiwan, primarily due to the high emission of air pollutants in the area. It is of note that the Daliao monitoring site is located less than 10 km from the coastal area in Kaohsiung, Taiwan.

Kaohsiung, an urban, agricultural and industrial metropolitan city in southern Taiwan, is the second largest city in the country. According to an emission inventory conducted by TEPA, emissions from the Kaohsiung air basin contributed over 20% to total air pollutant emissions in Taiwan (TEPA, 2005). The environmental loading of air pollutants in Kaohsiung was nearly twice that of other air basins in Taiwan (TEPA, 2006). Of the total emissions in Taiwan, 34,000 ton/yr $\text{PM}_{2.5}$, 157,000 ton/yr non-methane hydrocarbon, 66,000 ton/yr SO_x , and 164,000 ton/yr NO_x were emitted in the Kaohsiung area (TEPA, 2006). Seventy-eight percent of the air pollutants was emitted from stationary sources (power plant, oil refinery plant, iron and steel industry, petrochemical industry, and others) and 22% from mobile sources (motorcycles, gasoline vehicles, diesel vehicles and off-road vehicles) (TEPA, 2006). The location of the sampling site and emission sources is shown in Fig. 1.

Although particulate matter accounts for a large portion of the air pollution in this area, meteorological variations also influence bad air quality episodes. Generally, the rainy season runs from May to September (summer to autumn), and high-pollution episodes often occur between October and February (winter to spring) during the following year.

In Taiwan, the ambient air quality standard of 24 h PM_{10} concentration is set at $125 \mu\text{g}/\text{m}^3$. Therefore, the sampling concentration of $\text{PM}_{10} \geq 125 \mu\text{g}/\text{m}^3$ was presented as the episode days and the PM_{10} concentration $< 125 \mu\text{g}/\text{m}^3$ was presented as the non-episode days.

Sampling Program

In January, March, August and December 2006 and July 2007, there were 15 episode samples (with an average PM_{10} concentration of $163 \pm 30 \mu\text{g}/\text{m}^3$) and 23 non-episode samples (with an average PM_{10} concentration of $54 \pm 28 \mu\text{g}/\text{m}^3$) during which TEPA monitored for PM_{10} levels.

The sampling system used in this study consisted of a MOUDI and a nano-MOUDI sampler. This system has been used previously by many other investigators (e.g., Geller *et al.*, 2002; Miguel *et al.*, 2005). The designed cut-off sizes were 18, 3.2, 1.8, 1.0, 0.56, 0.32, 0.18, 0.10, 0.056, 0.032, 0.018, and 0.010 μm . The flow rates for MOUDI and nano-MOUDI were 30 and 10 L/min, respectively. Particulate matter was collected using 47-mm Teflon filters (ZeflurTM-supported PTFE) for the nano-MOUDI sampler and 37-mm filters for the MOUDI sampler. The weight of the filters and collected mass particulate concentration were measured using a microbalance (Mettler Toledo, MX5) with a reading precision of 3 μg at 25°C and 40% relative humidity. Prior to weighing, the filters were conditioned at $25 \pm 2^\circ\text{C}$ and $40 \pm 5\%$ relative humidity for 48 h.

Denuder Sampling

The denuder system employed in this study was composed of a cyclone with a cut-off diameter of 2.5 μm (University Research Glassware, URG, Chapel Hill Inc., USA) followed by four annular denuders (URG-2000-30EH), a filter pack, a flow controller and a pump (USEPA, 1998). Airflow was set at a constant rate of 16.7 L/min.

The first denuder was coated with 10 mL of 0.1% (w/v)

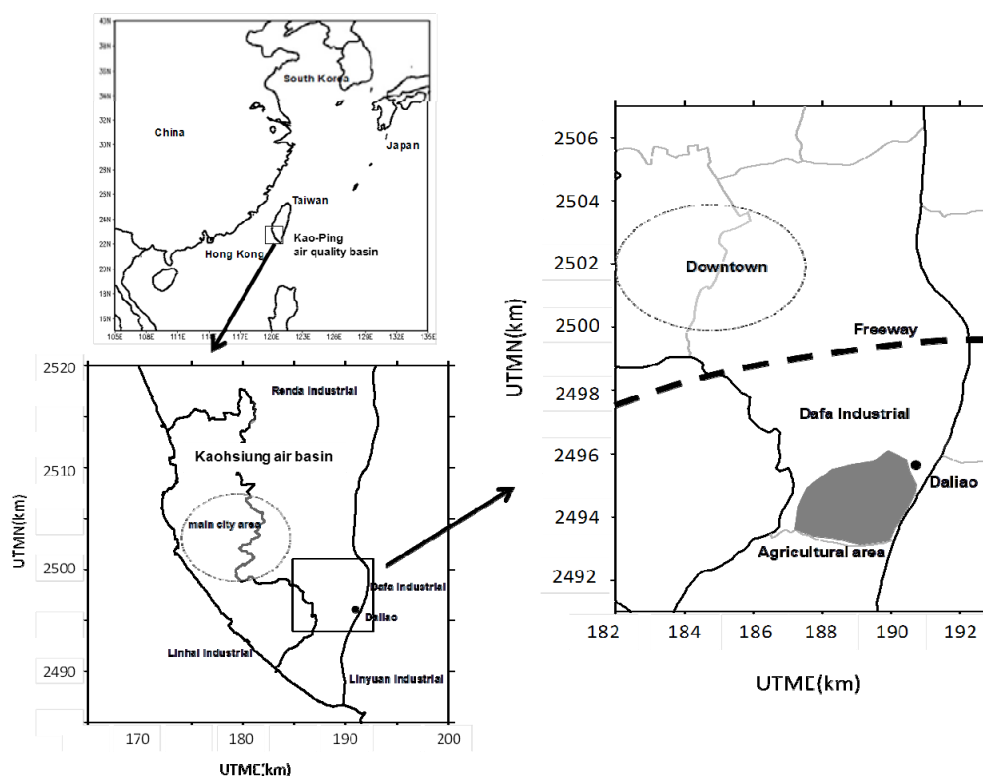


Fig. 1. Map of emission sources and sampling site.

NaCl in 1:9 methanol/deionized water solutions for the absorption of HNO_3 gas (Perrino *et al.*, 1990; USEPA, 1998). The second and third denuders were coated with 10 mL 1:1 (v:v) mixtures of 2% (w/v) Na_2CO_3 in deionized water and 2% (w/v) glycerol in methanol solution for the absorption of HCl , HNO_2 and SO_2 gas. The fourth was coated with 10 mL of 1% (w/v) citric acid in methanol solution for the absorption of NH_3 gas. Three filters placed in series followed the denuders. The first Teflon filter (Pallflex, 47 mm, pore size: 2 μm , USA) was set up to collect particulate matter < 2.5 μm in diameter. In order to collect acid gas that evaporated from particles or that was not completely absorbed by the denuder, the next quartz filter was coated with Na_2CO_3 solution. The last quartz filter was coated with a citric acid solution and designed to collect NH_3 evaporated from the particles. After sampling, each denuder tube and filter was extracted with deionized water and analyzed by ionic chromatography. Two denuder sampling systems were analyzed at Daliao station for quality assurance and quality control procedures, and the relative error for all gas species and particulate ions ranged from 5–17%. In addition, the additives of HNO_3 , SO_2 and NH_3 gases were used to measure the recovery of the denuder adsorption system. Recoveries were $97 \pm 6\%$, $96 \pm 5\%$ and $98 \pm 11\%$ for HNO_3 , SO_2 and NH_3 , respectively. The gas collection efficiency was similar to that reported in other studies (Sioutas *et al.*, 1996; Acker *et al.*, 2005).

Chemical Analysis

The collected aerosol filters were ultrasonically extracted for 2 h into 20 mL of deionized distilled water and passed

through a Teflon filter of 4.5 μm nominal pore size. Ion chromatography (Dionex, 120) was used to analyze the concentration of anions (Br^- , F^- , Cl^- , NO_2^- , NO_3^- , SO_4^{2-}) and cations (Na^+ , NH_4^+ , K^+ , Mg^{2+} , Ca^{2+}). The separation of anions was accomplished using an IonPac AS 12A (4 \times 200 mm) analytical column, an AG 14 guard column with a 10 μL sample loop, and an anion self-regenerating suppressor-ultra. A solution of 2.7 mM Na_2CO_3 /0.3 mM NaHCO_3 was used as an effluent at a flow rate of 1.5 mL/min. The separation of cations was accomplished using an IonPac CS 12A (4 \times 250 mm) analytical column, a CG 14 guard column with a 50 μL sample loop, and a cation self-regenerating suppressor-ultra. A solution of 20 mM methanesulfonic acid was used as the eluent at a flow rate of 1 mL/min. This analysis method yielded detection limits between 0.003 (Ca^{2+}) and 0.06 (NO_2^-) $\mu\text{g}/\text{m}^3$ and recoveries from 95 (Na^+) to 105% (NO_2^-). Some ionic imbalance was encountered due to carbonate species, especially in coarse particles when dust was abundant (Noguchi *et al.*, 2004; Hodzic *et al.*, 2006). The anion-to-cation charge ratio was in the range of 0.94 ± 0.13 in coarse particles. Therefore, the carbonate content did not seem to affect the ionic balance of particulate composition; however, the carbonate species were not examined in this work, which could be a limitation of the study.

RESULTS AND DISCUSSION

Particulate Matter Concentration

Particulate concentrations were 155 ± 32 and 46 ± 29 $\mu\text{g}/\text{m}^3$ on episode and non-episode days, respectively (Table 1). The mass concentration significantly increased in the

particle size ranges of 0.1–1.0 and 1.8–18 μm , and each size range contributed about 37–41% TSP mass concentration during episode and non-episode days. Generally, the chemical compositions of fine and coarse particles are distinct, and the processes affect the formation and removal of these two size fractions of aerosol in distinct ways. Fine particles are formed by nucleation with gases, while coarse particles are formed by mechanical processes from large particles. Distinct sources and production mechanisms generate modes of distinct chemical composition of fine and coarse particulate matter. Crustal (dust, minerals, sea salt) and biological material (pollen, spores, bacteria) could be the sources of coarse particles. Chemical reactions to form fine particulate matter, and sulfates, nitrates, ammonium, carbon, metals and water could be the composition of fine particles. Wind speed and relative humidity were not significantly different during the episode and non-episode days. But the temperatures were lower on episode days lower than on non-episode days, which could explain the bad air quality in winter and spring in southern Taiwan.

Particle size distributions for episode and non-episode days are shown in Fig. 2. PM mass did not increase in the nano and large particle sizes (D_p , particle aerodynamic diameter $> 18 \mu\text{m}$). But particulate number could be the

more important issue in nanoscale particulate matter. Due to their small size, nanoparticles make up a small fraction of the ambient particulate mass (less than 10%) but the majority of airborne particles by number. The major sources of primary nanoparticles are mobile vehicles and stationary fuel combustion in the South Coast Air Basin in California.

Water-soluble Ionic Species

Table 2 shows the ionic species content in different particulate sizes. Ionic species content ranged from 39 to 63% for episode days and from 14.5 to 39% for non-episode days. Results indicated that the high ionic species fraction contributed to particulate mass during the episode days and that the increase of ionic content was significant. Sulfate, nitrate, and ammonium were the major water-soluble species in PM constituents, contributing 70–90% of the mass fraction of analyzed ionic species at the particle size $> 1.0 \mu\text{m}$ and 50–60% mass concentration at the ultrafine particle size.

The $\text{PM}_{2.5}$ concentration and water-soluble ions identified in this study were compared to those of other studies conducted in southern Taiwan (Tsai and Chen *et al.*, 2006; Tsai *et al.*, 2011). Tsai and Chen's work (2006) indicated the concentrations of particulate matter and ionic constituents were in the same range for episode and non-episode periods

Table 1. PM mass concentration of different particle size during episode and non-episode periods.

Concentration ($\mu\text{g}/\text{m}^3$)	Episode (n = 15)	Non-episode (n = 23)	Ratio Episode/Non-episode
$\text{PM}_{>18}$	7.7 ± 4.5	2.4 ± 1.1	3.3
$\text{PM}_{1.8-18}$	57.8 ± 14.5	18.8 ± 8.1	3.1
$\text{PM}_{1-1.8}$	26.1 ± 12.2	5.4 ± 5.8	4.9
$\text{PM}_{0.1-1}$	57.9 ± 15.3	17.0 ± 14.1	3.4
$\text{PM}_{0.056-0.1}$	0.9 ± 0.5	0.4 ± 0.3	2.5
$\text{PM}_{0.056}$	4.5 ± 2.8	2.5 ± 2.2	1.9
TSP	155.0 ± 32.1	46.3 ± 28.8	3.4

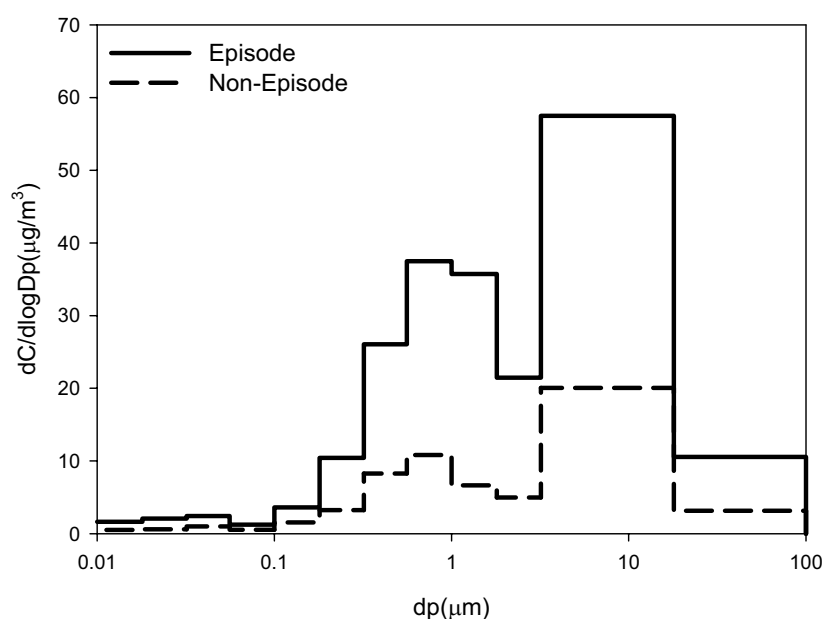


Fig. 2. Size distribution of particulate matter concentration on episode and non-episode days.

Table 2. Water-soluble ions in different particle size during episode and non-episode periods.

Concentration ($\mu\text{g}/\text{m}^3$)	Episode (n = 15)							
	TSP	PM ₁₈	PM _{1.8}	PM ₁	PM _{0.1}	PM _{nano}		
Na ⁺	3.05 ± 0.8	2.91 ± 0.8	0.97 ± 0.4	0.69 ± 0.3	0.19 ± 0.07	0.17 ± 0.06		
NH ₄ ⁺	15.27 ± 6.6	15.24 ± 6.6	13.03 ± 5.0	8.99 ± 2.9	0.19 ± 0.09	0.19 ± 0.18		
K ⁺	1.36 ± 0.4	1.33 ± 0.4	1.03 ± 0.3	0.79 ± 0.3	0.12 ± 0.07	0.11 ± 0.06		
Mg ²⁺	0.69 ± 0.2	0.64 ± 0.2	0.24 ± 0.1	0.17 ± 0.1	0.06 ± 0.02	0.05 ± 0.02		
Ca ²⁺	3.13 ± 1.0	2.84 ± 1.0	1.25 ± 0.7	0.93 ± 0.5	0.36 ± 0.21	0.32 ± 0.19		
Cl ⁻	4.23 ± 2.5	4.04 ± 2.5	2.27 ± 1.7	1.54 ± 1.0	0.20 ± 0.09	0.19 ± 0.08		
NO ₃ ⁻	28.70 ± 11.2	28.31 ± 11.2	19.11 ± 10.0	12.52 ± 5.7	0.36 ± 0.23	0.27 ± 0.12		
SO ₄ ²⁻	22.48 ± 6.4	22.23 ± 6.3	18.47 ± 5.6	13.57 ± 5.2	0.68 ± 0.43	0.54 ± 0.37		
Particulate Matter	155.0 ± 32.1	147.3 ± 33.5	89.4 ± 20.3	63.3 ± 14.9	5.4 ± 3.1	4.5 ± 2.7		

Concentration ($\mu\text{g}/\text{m}^3$)	Non-episode (n = 23)						PM _{2.5}	PM _{2.5}
	TSP	PM ₁₈	PM _{1.8}	PM ₁	PM _{0.1}	PM _{nano}	(Tsai and Chen, 2006)	(Tsai <i>et al.</i> , 2011)
Na ⁺	1.60 ± 0.6	1.46 ± 0.5	0.31 ± 0.1	0.19 ± 0.08	0.04 ± 0.03	0.05 ± 0.03	0.82–0.89	0.58–0.76
NH ₄ ⁺	2.57 ± 2.2	2.54 ± 2.2	2.16 ± 1.9	1.87 ± 1.58	0.05 ± 0.05	0.05 ± 0.02	3.91–5.10	2.12–4.21
K ⁺	0.38 ± 0.2	0.37 ± 0.2	0.26 ± 0.2	0.03 ± 0.03	0.02 ± 0.02	0.02 ± 0.02	1.00–1.42	0.57–0.62
Mg ²⁺	0.32 ± 0.1	0.30 ± 0.1	0.10 ± 0.04	0.07 ± 0.03	0.02 ± 0.02	0.02 ± 0.01	0.24–0.54	0.13–0.49
Ca ²⁺	0.88 ± 0.4	0.79 ± 0.4	0.28 ± 0.1	0.20 ± 0.10	0.04 ± 0.04	0.05 ± 0.05	0.93–1.34	0.54–0.66
Cl ⁻	1.72 ± 0.9	1.52 ± 0.8	0.28 ± 0.3	0.19 ± 0.23	0.02 ± 0.02	0.03 ± 0.02	1.31–1.37	1.06–1.07
NO ₃ ⁻	3.65 ± 3.6	3.53 ± 3.6	1.48 ± 1.8	1.14 ± 1.57	0.08 ± 0.09	0.08 ± 0.05	3.48–6.08	1.39–3.13
SO ₄ ²⁻	5.29 ± 3.7	5.20 ± 3.7	4.46 ± 3.4	3.81 ± 2.89	0.08 ± 0.07	0.06 ± 0.04	7.74–10.41	5.02–13.21
Particulate Matter	46.3 ± 28.8	43.9 ± 27.9	25.1 ± 20.6	19.8 ± 15.4	2.0 ± 2.2	2.5 ± 2.2	44–68	43–55

PM_x: particulate matter (PM) with diameter < x μm , and nano = 0.056 μm ; TSP: total suspended particle. n: sample number

of this study, but the sulfate and nitrate contents were about half of the values reported in our study. In addition, another work reported similar PM_{2.5} concentrations and compositions for non-episode periods but observed high chloride ion and sulfate content. This finding was attributed to the fact that their sampling site was near the coast (Tsai *et al.*, 2011).

During the episode periods, the sequence of the major ionic species in the fine particulate matter was NO₃⁻ > SO₄²⁻ > NH₄⁺ > Cl⁻ > Ca²⁺ > Na⁺ at the particulate size > 1.8 μm ; but the sequence was SO₄²⁻ > NO₃⁻ > NH₄⁺ > Cl⁻ > Ca²⁺ > Na⁺ > K⁺ at particulate size less than 1 μm . Results indicated that nitrate was higher than sulfate in coarse mode particles. But sulfate content was higher than nitrate content for particle size > 0.1 μm on non-episode days.

Na⁺, Ca²⁺ and Mg²⁺ predominated in the coarse particulate matter ($D_p > 1.8 \mu\text{m}$) (Figs. 3(a), (c) and (d)). This is consistent with work by Wall *et al.* (1988), which showed that sodium ions peak at around 1 to 10 μm and primarily in the coarse particulate matter. This is attributed to erosion of soil and crustal rock as well as sea salt spray. In this study, potassium ions (Fig. 3(b)) were dominant in the fine particles (0.18–1.8 μm) due to burning of vegetative material, i.e., rice straw, during the sampling period in Daliao, where there are some agricultural activities. Ryu *et al.* (2004) investigated biomass-burning aerosols and found that Cl⁻, NO₃⁻, SO₄²⁻, NH₄⁺, and K⁺ were the major ionic species in the particles. K⁺ is the major electrolyte in cell cytoplasm, which is released in large amounts of K-rich particulates in the submicron size fraction (Andrease *et al.*, 1983, 1998).

It is a useful tracer for pyrogenic aerosols in plants.

Xiu *et al.* (2004) also investigated inorganic ions in size-fractionated particulate matter and found that the sequence of concentration was SO₄²⁻ > NO₃⁻ \cong NH₄⁺ > Cl⁻ > F⁻ in each size fraction. According to the mass fraction of the ionic species, SO₄²⁻, NH₄⁺, and K⁺ were predominant in the fine particulate matter. Nitrate existed in both the fine and coarse particulate matter. In addition, SO₄²⁻ and NH₄⁺ were foremost in aerodynamic diameters less than 2 μm (fine particle) (Wall *et al.*, 1988). Wall *et al.* found that the nitrate peaks were in the aerodynamic diameters of 0.2, 0.7 and 3 μm , indicating that nitrate could form in fine and coarse modes.

High ammonium mass concentration was in the range of 0.18–3.2 μm , and most of the ammonium was in fine particles (< 1.8 μm) (Fig. 3(e)). In the atmosphere, NH₃ and HNO₃ are neutralized to form NH₄NO₃ in aerosol. Zhuang *et al.* (1999) investigated the production of ammonium from the condensation of NH₃ on particle surfaces. Ammonia reacts with acidic gases such as sulfuric acid, nitric acid and hydrochloric acid to form ammonium sulfate, ammonium nitrate and ammonium chloride in fine particles. Some suggested that the coarse mode ammonium resulted from the reaction of ammonia with acids such as sulfuric acid or nitric acid on the coarse particles (Wall *et al.*, 1998). The important sources of NH₃ are animal waste and ammonification of humus, followed by emission from soil, losses of NH₃-based fertilizers from soil, and industrial emissions in the area surrounding the sampling site.

The size distribution of chloride ion mass was significant in the size ranges of 0.32–1.8 and 3.2–18 μm (Fig. 3 (f)). Sea

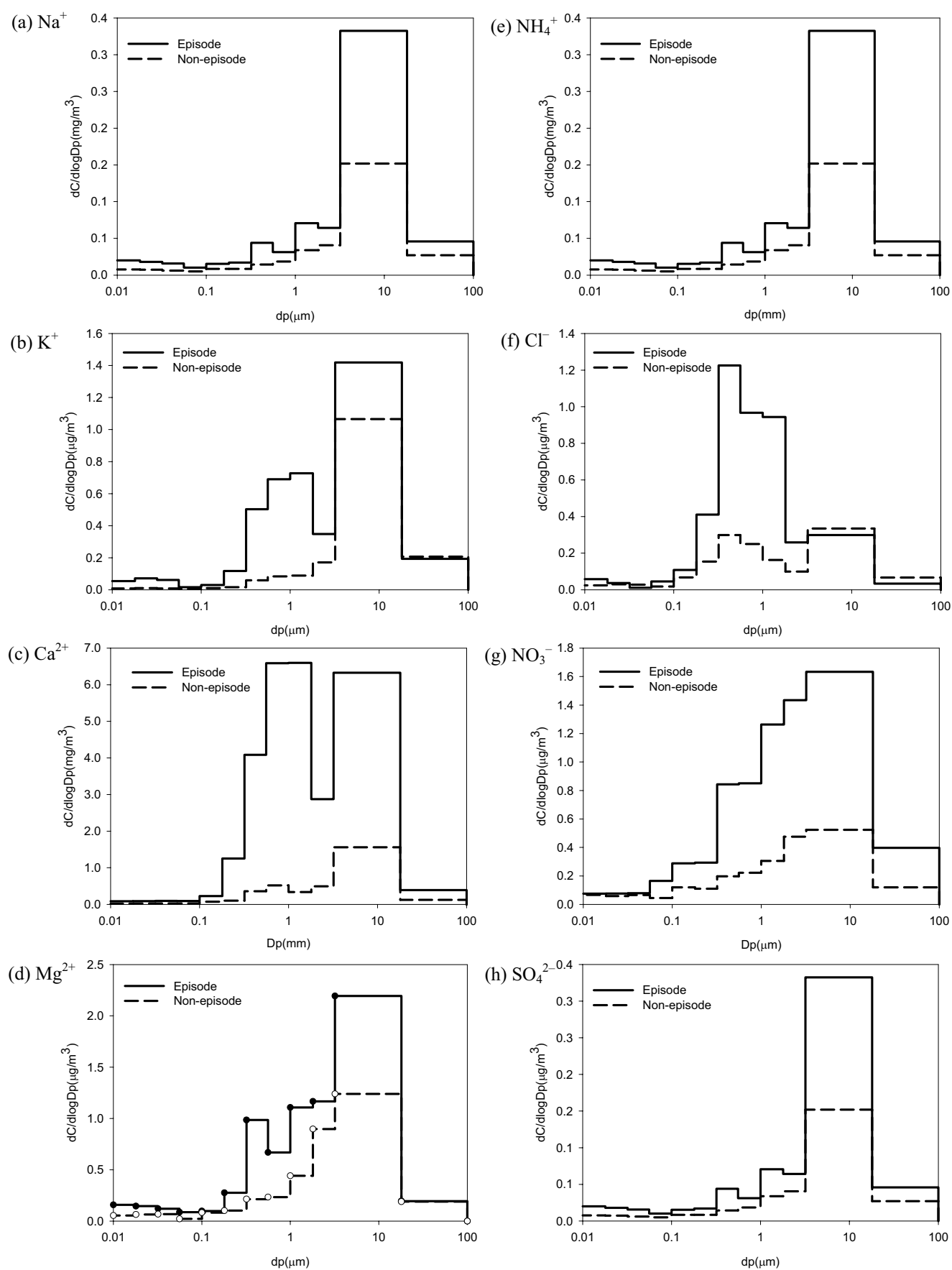


Fig. 3. Ionic species concentrations in different particulate matter size on episode and non-episode days.

salt could be the source of chloride ions in coarse particles, and industrial emissions and chemical reactions could be the source of fine particles.

Nitrate concentration peaks were bi-modal, one at the fine particle mode and the other at the coarse mode (Fig. 3(g)). About half of the NO_3^- is found in the coarse mode together with most of the Na^+ . The coarse mode- NO_3^- is the result of reactions of nitric acid (HNO_3) with sodium chloride or crustal material. De Leeuw *et al.* (2001) suggested that NaNO_3 is formed on the surface of an existing coarse mode sea salt or mineral dust particle, and NaNO_3 and $\text{Ca}(\text{NO}_3)_2$ can be collected in the coarse mode. A secondary aerosol is formed through the reaction of a natural sea salt or dust with anthropogenic HNO_3 . Jonson *et al.* (2000) reported that a large fraction of NO_3^- in sea salt was in the form of NaNO_3 due to its lower volatility than NH_4NO_3 .

Nitrate size distributions were bi-modal, peaking at 1.0–1.8 and 3.2–18 μm . During the episode periods, the nitrate in the 0.32–0.56 μm size range increased, and it could be formed by the co-condensation of gaseous ammonia and nitric acid on preexisting particles. Supermicron-mode nitrate (1.0–1.8 and 3.2–18 μm) could be formed through the reactions of gaseous nitric acid with sodium- or calcium-containing coarse particles.

NO_x can be converted into HNO_3 and combines with NH_3 to form nitrate as a secondary aerosol by photochemical reactions (Watson *et al.*, 1994; de Leeuw *et al.*, 2001). In this study, the nitrate concentration increased by about 8 times during the episode days; the precursor gas of NO_2 concentration ranged from 10 ppb on non-episode days to 32 ppb on episode days. Motor vehicle exhaust and stationary combustion sources could be the major sources of NO_x . Therefore, the increase of NO_2 could be one reason for the high concentration of NO_3^- in PM during the episode periods.

Kaneyasu *et al.* also found that nitrate and non-sea salt sulfate are predominant in fine particles because of local pollution (Kaneyasu *et al.*, 1999). Kaohsiung is an ozone non-attainment region and industrial metropolitan area, with power plants, industries (petrochemical industry, iron and steel plant etc.), and motor vehicles being the major sources of NO_x . Therefore, coal and oil combustion could be important sources of gaseous precursors of nitrate in fine particles.

In this study, the fine mode ($\text{dp} < 1.8 \mu\text{m}$) always dominated the distribution of sulfate (Fig. 3(h)). The peak of sulfate mass concentration was at 0.56–1.0 μm , and high concentration was found in the wide range from 0.1–18 μm . Neither condensation of vapor nor coagulation of smaller particulate matter was verified as the formation mechanism for particles less than 1 μm . Sulfate is most often converted from the photochemical oxidation of sulfur-containing precursors such as SO_2 , H_2S , CH_3SH , and CS_2 . SO_2 is the largest contributor of sulfate among the sulfur-containing compounds (Khoder, 2002). Sulfur oxide can be oxidized to H_2SO_4 by gas phase, aqueous phase, or multi-phase reactions of oxidants or radicals by condensation or nucleation of H_2SO_4 on particulate matter or to form a new aerosol. Partial H_2SO_4 was neutralized by NH_3 to form $(\text{NH}_4)_2\text{SO}_4$ or NH_4HSO_4 . In general, SO_4^{2-} is mainly in the fine particles,

particularly particles $< 1 \mu\text{m}$ (Zhuang *et al.*, 1999; Park and Kim, 2004), which is similar to the size distribution of sulfate in this study. Daliao sampling station is not far from the coastal area in Kaohsiung, Taiwan. Generally, the land-sea breeze extends inland about 30–100 km (Hsu, *et al.*, 1988; Chiu *et al.*, 2005; Muppa *et al.*, 2011). Therefore, sea salt and soil sulfate could be the sources of sulfate (Wall *et al.*, 1988; Zhuang *et al.*, 1999), especially in coarse particles (particulate diameter $> 2.5 \mu\text{m}$). In addition, the sulfate in coarse mode was attributed to the reaction of CaCO_3 with H_2SO_4 in aqueous phases to produce calcium sulfate (Davis and Jixiang, 2000; Xie *et al.*, 2005; Kouyoumdjian and Saliba, 2006). Furthermore, droplet oxidation of SO_2 in clouds was also suggested as a source of non-sea salt sulfate in coarse mode (Kerminen and Wexler, 1995).

Acid and Base Gases

Table 3 shows the acid and base gas concentrations; the average concentration of NH_3 was 27/25 $\mu\text{g}/\text{m}^3$, SO_2 was 26/6.6 $\mu\text{g}/\text{m}^3$, HNO_3 was 3.8/1.6 $\mu\text{g}/\text{m}^3$, HNO_2 was 6.0/2.6 $\mu\text{g}/\text{m}^3$, and HCl was 2.2/2.7 $\mu\text{g}/\text{m}^3$ during episode/non-episode periods. During the episode periods, the concentration of SO_2 , HNO_2 and HNO_3 increased significantly, but that of NH_3 did not. In addition, the NO_2 concentration was obtained from the TEPA, and its concentration was 18 $\mu\text{g}/\text{m}^3$ on non-episode days and increased to 61 $\mu\text{g}/\text{m}^3$ on episode days. The increase of NO_2 , HNO_2 and HNO_3 is associated with meteorological conditions that enhance the increase of NO_3^- in PM during episode periods. Compared to other areas, NH_3 was higher than in New York and Seoul, Korea; more agricultural activities could be one reason for the high concentration in Daliao. SO_2 concentration during the episode periods was high compared to other areas. HONO concentration was highest in Seoul, but HNO_3 was low.

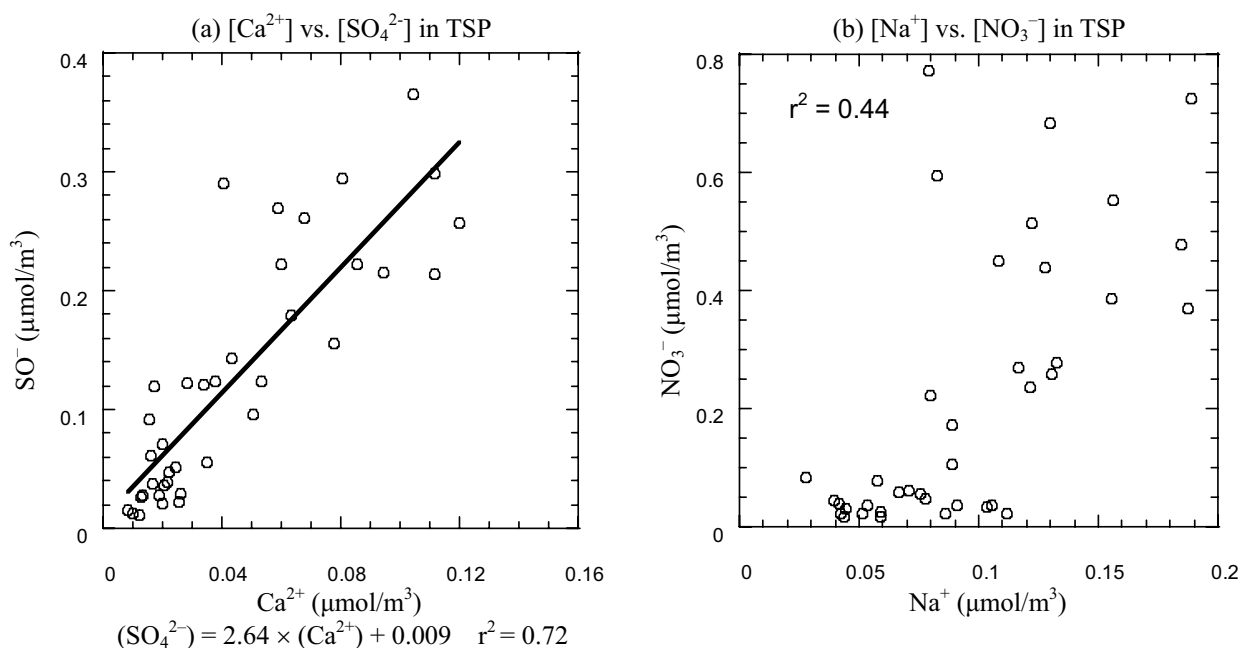
NO_2 reacts photochemically with hydroxyl radicals after sunrise and produces HNO_3 , which could be a dominant mechanism (Russell *et al.*, 1984, 1985). High HONO could come from combustion engines, i.e., diesel vehicles (Kurtenbach *et al.*, 2001), or heterogeneous reaction of NO_2 -HONO system (Su *et al.*, 2008; An *et al.*, 2009; Yu *et al.*, 2009). The HNO_2 could be rapidly photolyzed (wavelengths $\leq 400 \text{ nm}$) by “OH push” after sunrise and accumulated mostly at night (Platt and Perner, 1980; Calvert *et al.*, 1994; Staffelbach *et al.*, 1997; Acker *et al.*, 2005).

Ammonium, Nitrate and Sulfate System

High correlation was observed between calcium ions and sulfate at the larger particulate mode (Fig. 4(a)). But low correlation was found for two ionic species in fine particles (data not shown). In addition, low correlation was also observed between calcium ions and other species (Cl^- (correlation coefficient, $r < 0.6$), NO_3^- ($r < 0.7$)). Sulfate in the coarse mode may be attributed to the reaction of CaCO_3 with H_2SO_4 to form CaSO_4 in coarse particles (Davis and Jixiang, 2000; Xie *et al.*, 2005; Kouyoumdjian and Saliba, 2006). In addition, low correlations were determined between sodium ions and other anions such as chloride ions ($r < 0.6$), nitrate ($r < 0.7$) and sulfate ($r < 0.7$) at the larger particle size. Fig. 4(b) presented the correlation of sodium ions and nitrate

Table 3. Acid and base gas concentration ($\mu\text{g}/\text{m}^3$).

Site	Sampling periods		HCl	HNO ₂	HNO ₃	SO ₂	NH ₃	Remark
Daliao, Taiwan	2006.1–2007.7	Episode Non-episode	2.25 ± 2.46 2.68 ± 2.82	5.98 ± 2.98 2.63 ± 1.65	3.83 ± 3.69 1.60 ± 1.65	25.94 ± 11.32 6.55 ± 6.76	27.31 ± 11.07 25.35 ± 13.88	This study
Taichung, Taiwan	2002.1–2002.12		—	1.9–3.5	1.1–2.6	—	6.4–11.4	
New York, USA	1999.7–2000.6		0.25–0.93	1.92–4.44	0.62–3.58	17.55–40.60	2.85–4.24	Bari et al., 2003
Seoul, Korea	2001.10–2001.11	Hazy episodes Non-hazy episodes	—	11.4 ± 4.61 5.87 ± 1.81	0.94 ± 0.40 0.45 ± 0.14	8.68 ± 2.33 5.39 ± 1.66	6.00 ± 1.33 4.81 ± 1.78	Kang et al., 2004

**Fig. 4.** Characteristics of calcium ions, sodium ions, sulfate and nitrate in total suspended particles.

in TSP. Although some studies reported in the literature indicated that nitric acid could react with sodium chloride on sea salt aerosols (Tenbrink, 1998; Pryor and Sørensen, 2000; Saul et al., 2006), it was not express the high correlation between sodium ion and nitrate in the larger size range particles.

Based on the molar concentration of ammonium and sulfate at $\text{PM}_{0.1}$, the molar ratio of $[\text{SO}_4^{2-}]/[\text{NH}_4^+]$ was 0.54, and high correlation was observed between sulfate and ammonium in ultrafine mode (Fig. 5(a)). Results indicated that ammonium could neutralize sulfate to form $(\text{NH}_4)_2\text{SO}_4$ in the ultrafine mode.

In addition, nitrate came from both primary and secondary sources, with the coarse mode nitrate generated from sea salt spray and the fine mode nitrate produced by photochemical reaction. A strong correlation of ammonium and nitrate was determined at PM_1 (Fig. 5(b)). Furthermore, the equivalent ratio of $\{[\text{NO}_3^-] + [\text{SO}_4^{2-}]\}/[\text{NH}_4^+]$ was about 0.99 and revealed a high correlation between $\{[\text{NO}_3^-] + [\text{SO}_4^{2-}]\}$ and $[\text{NH}_4^+]$ that clearly pointed to ammonium neutralization or reaction with nitrogen and sulfur species to form ammonium nitrate and ammonium sulfate in PM_1 (Fig. 5(c)). Results indicated that ammonium nitrate and ammonium sulfate

could be the dominant constituents in the particle size $< 1 \mu\text{m}$. Solar radiation induces photochemical reactions that create hydroxyl radicals, which react with atmospheric constituents. Emissions of precursor gases (e.g., SO_2 , NO_x , NH_3) convert and react to ammonium nitrate (NH_4NO_3), ammonium sulfate ($(\text{NH}_4)_2\text{SO}_4$), and ammonium bisulfate (NH_4HSO_4) in the particulate phase.

For the nuclei mode, the SO_2 was significantly correlated to the SO_4^{2-} ($\text{PM}_{0.1}$) in the sulfur system (Fig. 5(d)). This could indicate that sulfur dioxide was transferred into the sulfate by chemical reaction. Therefore, the gas transfer reaction to particles could be the dominant pathway of SO_2 to form SO_4^{2-} , especially in the particle sizes characteristic of the nuclei mode.

CONCLUSIONS

Average PM mass concentration was about three times higher during episode periods ($155 \mu\text{g}/\text{m}^3$) than non-episode periods ($46 \mu\text{g}/\text{m}^3$), and the mass increased in the size ranges of 0.1–1.0 and 1.8–18 μm . Sulfate, nitrate and ammonium were the major ionic species in PM. Nitrate size distributions were bi-modal; sulfate concentration distribution revealed

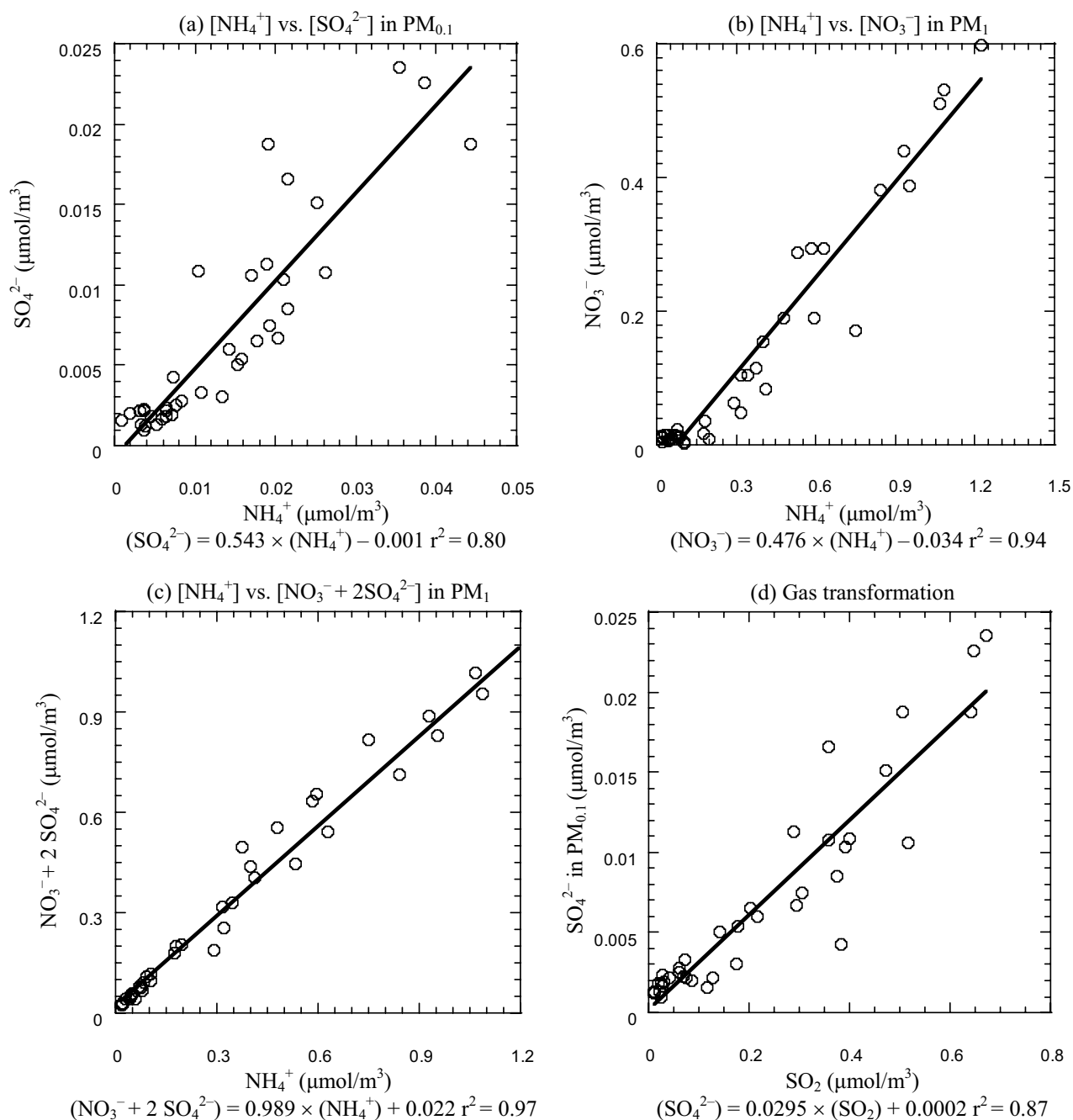


Fig. 5. Characteristics of gas and ionic species in particulate matter.

one mode and a wide range from 0.1–18 μm , and high ammonium mass concentration was in the range of 0.18–3.2 μm . In addition, the molar ratio of $[\text{SO}_4^{2-}]/[\text{NH}_4^+]$ was about 0.54, and a high correlation was observed between sulfate and ammonium at PM_{0.1}; results indicated $(\text{NH}_4)_2\text{SO}_4$ formed in the ultrafine mode. High SO_2 , NO_2 , HNO_3 , and HNO_2 were observed during episode periods. Furthermore, SO_2 was significantly correlated to PM- SO_4^{2-} (PM_{0.1}), which implied a gas transfer reaction in the nuclei mode aerosol.

ACKNOWLEDGEMENTS

The authors acknowledge the supports of National Science

Council, Taiwan (NSC 94-2211-E-006-087, NSC 95-2211-E-006-287, NSC 96-2211-E-006-004).

REFERENCES

- Acker, K., Möller, D., Auel, R., Wiprecht, W. and Kalaß, D. (2005). Concentration of Nitrous Acid, Nitric Acid, Nitrite and Nitrate in the Gas and Aerosol Phase at a Site in the Emission Zone during ESCOMPTE 2001 Experiment. *Atmos. Res.* 74: 507–524.
- An, J., Zhang, W. and Qu, Y. (2009). Impacts of a Strong Cold Front on Concentrations of HONO, HCHO, O_3 and NO_2 in the Heavy Traffic Urban Area of Beijing. *Atmos.*

- Environ.* 43: 3454–3459.
- Andrease, M.O. (1983) Soot Carbon and Excess Fine Potassium: Long-Range Transport of Combustion-Derived Aerosols. *Science* 220: 1148–1151.
- Andrease, M.O., Andreae, T.W., Annegarn, H., Beer, J., Cachier, H., Canut, P., Elbert, W., Maenhaut, W., Salma, I., Wienhold, F.G. and Zenker, T. (1998) Airborne Studies of Aerosol Emissions from Savanna Fires in Southern Africa: 2. Aerosol Chemical Compositions. *J. Geophys. Res.* 109: 32119–32128.
- Aneja, V.P., Wang, B., Tong, D.Q., Kimball, H. and Steger, J. (2006). Characterization of Major Chemical Components of Fine Particulate Matter in North Carolina. *J. Air Waste Manage. Assoc.* 56: 1099–1107.
- Bari, A., Dutkiewicz, V.A., Judd, C.D., Wilson, L.R., Luttinger, D. and Husain, L. (2003b). Regional Sources of Particulate Sulfate, SO₂, PM_{2.5}, HCl, and HNO₃, in New York, NY. *Atmos. Environ.* 37: 2837–2844.
- Bari, A., Ferraro, V., Wilson, L.R., Luttinger, D. and Husain, L. (2003a). Measurements of Gaseous HONO, HNO₃, SO₂, HCl, NH₃, Particulate Sulfate and PM_{2.5} in New York, NY. *Atmos. Environ.* 37: 2825–2835.
- Boldo, E., Linares, C., Lumbreras, J., Borge, R., Narros, A., García-Pérez, J., Fernández-Navarro, P., Pérez-Gómez, B., Aragonés, N., Ramis, R., Pollán, M., Moreno, T., Karanasiou, A. and López-Abente, G. (2011). Health Impact Assessment of a Reduction in Ambient PM_{2.5} Levels in Spain. *Environ. Int.* 37: 342–348.
- Brunekreef, B. and Forsberg, B. (2005). Epidemiological Evidence of Effects of Coarse Airborne Particles on Health. *Eur. Respir. J.* 26: 309–318.
- Brunekreef, B., Beelen, R., Hoek, G., Schouten, L., Bausch-Goldbohm, S., Fischer, P., Armstrong, B., Hughes, E., Jerrett, M. and van den Brandt, P. (2009). Effects of Long-Term Exposure to Traffic-Related Air Pollution on Respiratory and Cardiovascular Mortality in the Netherlands: The NLCS-AIR Study. *Res. Rep. Health Eff. Inst.* 139: 5–71.
- Buhr, S.M., Buhr, M.P., Fehsenfeld, F.C., Holloway, J.S., Karst, U., Norton, R.B., Parrish, D.D. and Sievers, R.E. (1995). Development of a Semi-Continuous Method for the Measurement of the Nitric Acid Vapor and Particulate Nitrate and Sulfate. *Atmos. Environ.* 29: 2609–2624.
- Burnett, R.T., Cakmak, S., Brook, J.R. and Krewski, D. (1997). The Role of Particulate Size and Chemistry in the Association between Summertime Ambient Air Pollution and Hospitalization for Cardiorespiratory Disease. *Environ. Health Perspect.* 105: 614–620.
- Cabada, J.C., Rees, S., Takahama, S., Khlystov, A., Pandis, S.N., Davidson, C.I. and Robinson, A.L. (2004). Mass Size Distribution and Size Resolved Chemical Composition of Fine Particulate Matter at Pittsburgh Supersite. *Atmos. Environ.* 38: 3127–3141.
- Calvert, J.G., Yarwood, G. and Dunker, A. (1994). An Evaluation of the Mechanism of Nitrous Acid Formation in the Urban Atmosphere. *Res. Chem. Intermed.* 20: 463–502.
- Chiu, K.H., Sree, U., Tseng, S.H., Wu, C.H. and Lo, J.G. (2005). Differential Optical Absorption Spectrometer Measurement of NO₂, SO₂, O₃, HCHO and Aromatic Volatile Organics in Ambient Air of Kaohsiung Petroleum Refinery in Taiwan. *Atmos. Environ.* 39: 941–955.
- Davis, B. and Jixiang, G. (2000). Airborne Particulate Study in Five Cities of China. *Atmos. Environ.* 34: 2703–2711.
- de Leeuw, G., Cohen, L., Frohn, L.M., Geernaert, G., Hertel, O., Jensen, B., Jickells, T., Klein, L., Kunz, G.J. and Lund, S. (2001). Atmospheric Input of Nitrogen into North Sea: ANICE Project Overview. *Cont. Shelf Res.* 21: 2073–2094.
- Deshmukh, D.K., Deb, M.K., Tsai, Y.I. and Mkoma, S.L., (2011). Water Soluble Ions in PM_{2.5} and PM₁ Aerosols in Durg City, Chhattisgarh, India. *Aerosol Air Qual. Res.* 11: 696–708.
- Geller, M.D., Kim, S., Misra, C., Sioutas, C., Olson, B.A. and Marple, V.A. (2002). A Methodology for Measuring Size-Dependent Chemical Composition of Ultrafine Particles. *Aerosol Sci. Technol.* 36: 748–762.
- Han, S., Bian, H., Zhang, Y., Wu, J., Wang, Y., Tie, X., Li, Y., Li, X. and Yao, Q. (2012). Effect of Aerosols on Visibility and Radiation in Spring 2009 in Tianjin, China. *Aerosol Air Qual. Res.* 12: 211–217.
- Han, Y.J., Kim, T.S. and Kim, H. (2008). Ionic Constituents and Source Analysis of PM_{2.5} in Three Korea Cities. *Atmos. Environ.* 42: 3127–3141.
- Hazi, Y., Heikkinen, M.S.A. and Cohen, B.S. (2003). Size Distribution of Acidic Sulfate Ions in Fine Ambient Particulate Matter and Assessment of Source Region Effect. *Atmos. Environ.* 37: 5403–5413.
- Health Effects Institute (2003). Revised Analyses of the National Morbidity, Mortality and Air Pollution Study, Part II: Revised Analyses of Selected Time-Series Studies of Air Pollution and Health, Cambridge, MA: Health Effects Institute.
- Hodzic, A., Bessagnet, B. and Vautard, R. (2006). A Model Evaluation of Coarse-Mode Nitrate Heterogeneous Formation on Dust Particles. *Atmos. Environ.* 40: 4158–4171.
- Hsieh, L.Y., Kuo, S.C., Chen, C.L. and Tsai, Y.I. (2009). Size Distribution of Nano/Micro Dicarboxylic Acids and Inorganic Ions in Suburban PM Episode and Non-Episodic Aerosol. *Atmos. Environ.* 43: 4396–4406.
- Hsu, S.A. (1988). *Coastal Meteorology*, Academic Press, San Diego.
- Hu, D., Qiao, L., Chen, J., Ye, X., Yang, X., Cheng, T. and Fang, W. (2010). Hygroscopicity of Inorganic Aerosols: Size and Relative Humidity Effects on the Growth Factor. *Aerosol Air Qual. Res.* 10: 255–264.
- Jonson, J.E., Semb, A., Barrett, K., Grini, A. and Tarrason, L. (Ed.) On the Distribution of Sea Salt and Sodium Nitrate Particles in Europe, Transport and Chemical Transportation in Troposphere, Proc. of the EUROTRAC Symposium Sixth, Gaimisch-Partenkirchen, Germany, 2000, p. 695–699.
- Kan, H., London, S.J., Chen, G., Zhang, Y., Song, G., Zhao N., Jiang, L. and Chen, B. (2007). Differentiating the Effects of Fine and Coarse Particles on Daily Mortality in Shanghai, China. *Environ. Int.* 33: 376–384.
- Kaneyasu, N., Yoshikado, H., Mizuno, T., Sakamoto, K. and Soufuku, M. (1999). Chemical Forms and Sources

- of Extremely High Nitrate and Chloride in Winter Aerosol Pollution in the Kanto Plain of Japan. *Atmos. Environ.* 33: 1745–1756.
- Kang, C.M., Lee, H.S., Kang, B.W., Lee, S.K. and Sunwoo, Y. (2004). Chemical Characteristics of Acidic Gas Pollutants and PM_{2.5} Species during Hazy Episodes in Seoul, South Korea. *Atmos. Environ.* 38: 4749–4760.
- Katzman, T.L., Rutter, A.P., Schauer, J.J., Lough, G.C., Kolb, C.J. and Klooster, S.V. (2010). PM_{2.5} and PM_{10–2.5} Compositions during Wintertime Episodes of Elevated PM Concentrations across the Midwestern USA. *Aerosol Air Qual. Res.* 10: 143–150.
- Kerminen, V.M. and Wexler, A.S. (1995). Growth Laws for Atmospheric Aerosol Particle: An Examination of Bimodality of the Accumulation Mode. *Atmos. Environ.* 29: 3263–3275.
- Khoder, M.I. (2002). Atmospheric Conversion of Sulfur Dioxide to Particulate Sulfate and Nitrogen Dioxide to Particulate Nitrate and Gaseous Nitric Acid in an Urban Area. *Chemosphere* 49: 675–684.
- Kouyoumdjian, H. and Saliba, N.A. (2006). Mass Concentration and Ion Concentration of Coarse and Fine Particles in an Urban Area in Beirut: Effect of Calcium Carbonate on the Absorption of Nitric and Sulfuric Acids and the Depletion of Chloride. *Atmos. Chem. Phys.* 6: 1865–1877.
- Kurtenbach, R., Becker, K.H., Gomes, J.A.G., Kleffmann, J., Lörzer, J.C., Spittler, M., Wiesen, P., Ackermann, R., Geyer, A. and Platt, U. (2001). Investigations of Emissions and Heterogeneous Formation of HONO in a Road Traffic Tunnel. *Atmos. Environ.* 35: 3385–3394.
- Lee, H.S., Kang, C.M., Kang, B.W. and Kim, H.K. (1999). Seasonal Variations of Acidic Air Pollutants in Seoul, South Korea. *Atmos. Environ.* 33: 3143–3152.
- Li, W., Bai, Z., Liu, A., Chen, J. and Chen, L. (2009). Characteristics of Major PM_{2.5} Components during Winter in Tianjin, China. *Aerosol Air Qual. Res.* 9: 105–119.
- Lin, C.C., Huang, K.L., Chen, S.J., Liu, S.C., Tsai, J.H., Lin, Y.C. and Lin, W.Y. (2009). NH₄⁺, NO₃[–] and SO₄^{2–} in Roadside and Rural Size-Resolved Particles and Transformation of NO₂/SO₂ to Nanoparticle-Bound NO₃[–]/SO₄^{2–}. *Atmos. Environ.* 43: 2731–2736.
- Miguel, A.H., Eiguren-Fernandez, A., Sioutas, C., Fine, P.M., Geller, M. and Mayo, P.R. (2005). Observation of Twelve USEPA Priority Polycyclic Aromatic Hydrocarbons in the Aitken Size Range (10–32 nm Dp). *Aerosol Sci. Technol.* 39: 415–418.
- Muppa, S.K., Anandan, V.K., Kesarkar, K.A., Rao, S.V.B. and Reddy, P.N. (2011). Study on Deep Inland Penetration of Sea Breeze over Complex Terrain in the Tropics. *Atmos. Res.* 104–105: 209–216.
- Naess, O., Piro, F.N., Naftstad, P., Smith, G.D. and Leyland, A.H. (2007). Air Pollution, Social Deprivation and Mortality: A Multilevel Cohort Study. *Epidemiology* 18: 686–694.
- Noguchi, I. and Hara, H. (2004). Ionic Imbalance Due to Hydrogen Carbonate from Asian Dust. *Atmos. Environ.* 38: 6969–6976.
- Ny, M.T. and Lee, B.K. (2011). Size Distribution of Airborne Particulate Matter and Associated Metallic Elements in an Urban Area of an Industrial City in Korea. *Aerosol Air Qual. Res.* 11: 643–653.
- Oberdorster, G., Gelein, R.M., Ferin, J. and Weiss, B. (1995). Association of Particulate Air Pollution and Acute Mortality: Involvement of Ultra-fine Particles? *Inhal. Toxicol.* 7: 111–124.
- Oh, M.S., Lee, T.J. and Kim, D.S. (2011). Quantitative Source Apportionment of Size-segregated Particulate Matter at Urbanized Local Site in Korea. *Aerosol Air Qual. Res.* 11: 247–264.
- Ostro, B.D., Broadwin, R. and Lipsett, M.J. (2000). Coarse and Fine Particles and Daily Mortality in the Coachella Valley, California: A Follow-up Study. *J. Exposure Anal. Environ. Epidemiol.* 10: 412–419.
- Park, S.S. and Kim, Y.J. (2004). PM_{2.5} Particles and Size-segregated Ionic Species Measured during Fall Season in Three Urban Sites in Korea. *Atmos. Environ.* 38: 1459–1471.
- Pathak, R.K. and Chan, C.K. (2005). Inter-Particle and Gas-Particle Interactions in Sampling Artifacts of PM_{2.5} in Filter-Based Samplers. *Atmos. Environ.* 39: 1597–1607.
- Pathak, R.K., Yao, X. and Chan, C.K. (2004). Sampling Artifacts of Acidity and Ionic Species in PM_{2.5}. *Environ. Sci. Technol.* 38: 254–259.
- Pathak, R.K., Yao, X., Lau, A.K.H. and Chan, C.K. (2003). Acidity and Concentrations of Ionic Species of PM_{2.5} in Hong Kong. *Atmos. Environ.* 37: 1113–1124.
- Perrino, C., DeSantis, F. and Febo, A. (1990). Criteria for the Choice of a Denuder Sampling Technique Devoted to the Measurement of Atmospheric Nitrous and Nitric Acids. *Atmos. Environ.* 24A: 617–626.
- Platt, U. and Perner, D. (1980). Direct Measurements of Atmospheric CH₂O, HNO₂, O₃, NO₂ and SO₂ by Differential Optical Absorption in the Near UV. *J. Geophys. Res.* 85: 7453–7458.
- Plaza, J., Pujadas, M., Gómez-Moreno, F.J., Sánchez, M. and Artíñano, B. (2011). Mass Size Distribution of Soluble Sulfate, Nitrate and Ammonium in the Madrid Urban Aerosol. *Atmos. Environ.* 45: 4966–4976.
- Plessow, K., Spindler, G., Zimmermann, F. and Matschullat, J. (2005). Seasonal Variations and Interactions of N-Containing Gases and Particles over a Coniferous Forest, Saxony, Germany. *Atmos. Environ.* 39: 6995–7007.
- Pryor, S.C. and Sørensen, L.L. (2000). Nitric Acid-Sea Salt Reactions: Implications for Nitrogen Deposition to Water Surface. *Bull. Am. Meteorol. Soc.* 39: 725–731.
- Russell, A.G., McRae, G.J. and Cass, G.R. (1984). Acid Deposition of Photochemical Oxidation Products—a Study Using a Lagrangian Trajectory Models, In *Air Pollution Modeling and its Application III*, De Wispelaere, C. (Ed.), Plenum Press, New York, p. 539–564.
- Russell, A.G., McRae, G.J. and Cass, G.R. (1985). The Dynamics of Nitric Acid Production and the Fate of Nitrogen Oxides. *Atmos. Environ.* 19: 893–902.
- Ryu, S.Y., Kim, J.E., Zhuanshi, H., Kim, Y.J. and Kang, G.U. (2004). Chemical Composition of Post-Harvest Biomass Burning Aerosols in Gwangju, Korea. *J. Air Waste Manage. Assoc.* 54: 1124–1137.

- Saul, T.D., Tolocka, M.P. and Johnston, M.V. (2006). Reaction Uptake of Nitric Acid onto Sodium Chloride Aerosols across a Wide Range of Reactive Humidity. *J. Phys. Chem. A* 110: 7614–7620.
- Shen, Z., Cao, J., Tong, Z., Liu, S., Reddy, L.S.S., Han, Y., Zhang, T. and Zhou, J. (2009). Chemical Characteristics of Submicron Particles in Winter in Xi'an. *Aerosol Air Qual. Res.* 9: 80–93.
- Shen, Z., Wang, X., Zhang, R., Ho, K., Cao, J. and Zhang, M. (2011). Chemical Composition of Water-soluble Ions and Carbonate Estimation in Spring Aerosol at a Semi-arid Site of Tongyu, China. *Aerosol Air Qual. Res.* 11: 360–368.
- Sioutas, C., Wang, P.Y., Ferguson, S.T., Koutrakis, P. and Mulik, J.D. (1996). Laboratory and Field Evaluation of an Improved Glass Honeycomb Denuder/Filter Pack Sampler. *Atmos. Environ.* 30: 885–895.
- Staffelbach, T., Neftel, A. and Horowitz, L.W. (1997). Photochemical Oxidant Formation over Southern Switzerland: 2. Model Results. *J. Geophys. Res.* 102: 23363–23373.
- Stone, E.A., Yoon, S.C. and Schauer, J.J. (2011). Chemical Characterization of Fine and Coarse Particles in Gosan, Korea during Springtime Dust Events. *Aerosol Air Qual. Res.* 11: 31–43.
- Su, H., Cheng, Y.F., Cheng, P., Zhang, Y.H., Dong, S., Zeng, L.M., Wang, X., Slanina, J., Shao, M. and Wiedensohler, A. (2008). Observation of Nighttime Nitrous Acid (HONO) Formation at a Non-Urban Site during PRIDE-PRD2004 in China. *Atmos. Environ.* 42: 6219–6232.
- Taiwan Environmental Protection Agency (TEPA) (2005). Air Pollutants Emission Database and Air Quality Management Program, EPA-94-FA11-030-A139, Taipei, Taiwan.
- Tenbrink, H. (1998). Reactive Uptake of HNO_3 and H_2SO_4 in Sea-Salt (NaCl) Particles. *J. Aerosol Sci.* 29: 57–64.
- TEPA (2006). Emission of Air Pollutants in Taiwan- Taiwan Emission Data System (TEDS 6.1), Taipei. (in Chinese)
- Tsai, H.H., Yuan, C.S., Hung, C.H. and Lin C. (2011). Physicochemical Properties of $\text{PM}_{2.5}$ and $\text{PM}_{2.5-10}$ at Inland and Offshore Sites over Southeastern Coastal Region of Taiwan Strait. *Aerosol Air Qual. Res.* 11: 664–678.
- Tsai, J.H., Lin J.J., Chiang, H.L., Chang, K.L. and Lin, Y. H. (2005). Mass-Size Distributions of Particulate Sulfate, Nitrate, and Ammonium in PM Non-attainment Region in Southern Taiwan. *J. Air Waste Manage. Assoc.* 55: 502–509.
- Tsai, Y.I. and Chen, C.L. (2006). Characterization of Asian Dust Storm and Non-Asian Dust Storm $\text{PM}_{2.5}$ Aerosol in Southern Taiwan. *Atmos. Environ.* 40: 4734–4750.
- Tsai, Y.I. and Kuo, S.C. (2006). Development of Diffuse Reflectance Infrared Fourier Transform Spectroscopy for the Rapid Characterization of Aerosols. *Atmos. Environ.* 40: 1781–1793.
- USEPA (1998). Compendium of Methods for the Determination of Inorganic Compounds in Ambient Air –IO-4.2 Determination of Reactive Acid and Basic Gases and Strong Acidity in Fine Particles, USEPA Publication 625/R-96/010a, Cincinnati, OH.
- Walker, J.T., Whittall, D.R., Robarge, W. and Paerl, H.W. (2003). Ambient Ammonia and Ammonium Aerosol across a Region of Variable Ammonia Emission Density. *Atmos. Environ.* 38: 1235–1246.
- Wall, S.M., John, W. and Ondo, J.L. (1998). Measurement of Aerosol Size Distributions for Nitrate and Major Ionic Species. *Atmos. Environ.* 22: 1649–1656.
- Wang, C.F., Chang, Z.Y., Tsai, S.F. and Chiang, H.L. (2005). Characteristics of Road Dust from Different Sampling Sites in Northern Taiwan. *J. Air Waste Manage. Assoc.* 55: 1236–1244.
- Wang, W.C., Chen, K.S., Chen, S.J., Lin, C.C., Tsai, J.H. Lai, C.H. and Wang, S.K. (2008). Characteristics and Receptor Modeling of Atmospheric $\text{PM}_{2.5}$ at Urban and Rural Sites in Pingtung, Taiwan. *Aerosol Air Qual. Res.* 8: 112–129.
- Watson, J.G., Chow, J.C., Lurmann, F.W. and Musarra, S.P. (1994). Ammonium Nitrate, Nitric Acid, and Ammonia Equilibrium in Wintertime Phoenix, Arizona. *J. Air Waste Manage. Assoc.* 44: 405–412.
- Xie, R.K., Seip, H.M., Leinum, J.R., Winje, T. and Xiao, J.S. (2005). Chemical Characterization of Individual Particles (PM_{10}) from Ambient Air in Guiyang City, China. *Sci. Total Environ.* 343: 261–272.
- Xiu, G., Zhang, D., Chen, J., Huang, X., Chen, Z., Guo, H. and Pan, J. (2004). Characterization of Major Water-Soluble Inorganic Ions in Size-Fractionated Particulate Matters in Shanghai Campus Ambient Air. *Atmos. Environ.* 38: 227–236.
- Ying, Q. and Kleeman, M.J. (2006). Source Contributions to the Regional Distribution of Secondary Particulate Matter in California. *Atmos. Environ.* 40: 736–752.
- Yu, Y., Galle, B., Panday, A., Hodson, E., Prinn, R. and Wang, S. (2009). Observations of High Rates of NO_2 -HONO Conversion in the Nocturnal Atmospheric Boundary Layer in Kathmandu, Nepal. *Atmos. Chem. Phys.* 9: 6401–6415.
- Zhao, J., Zhang, F., Xu, Y., Chen, J., Yin, L., Shang, X. and Xu, L. (2011). Chemical Characteristics of Particulate Matter during a Heavy Dust Episode in a Coastal City, Xiamen, 2010. *Aerosol Air Qual. Res.* 11: 299–308.
- Zhao, Y. and Gao, Y. (2008). Mass Size Distributions of Water-Soluble Inorganic and Organic Ions in Size-Segregated Aerosols over Metropolitan Newark in the US East Coast. *Atmos. Environ.* 42: 4063–4078.
- Zhuang, H., Chan, C.K., Fang, M. and Wexler, A.S. (1999). Size Distributions of Particulate Sulfate, Nitrate, and Ammonium at a Coastal Site in Hong Kong. *Atmos. Environ.* 33: 843–853.

Received for review, October 9, 2011

Accepted, December 5, 2011